Improving the lifetime in optical microtraps by using elliptically polarized dipole light

Sébastien Garcia, Jakob Reichel, Romain Long

Improving the lifetime in optical microtraps by using elliptically polarized dipole light

Sébastien Garcia,[1, 2, *] Jakob Reichel,[1] and Romain Long[1, †]

[1] *Laboratoire Kastler Brossel, ENS-PSL Research University, CNRS, UPMC-Sorbonne Universités, Collège de France, 24 rue Lhomond, 75005 Paris, France*

[2] *Department of Physics, ETH Zürich, CH-8093 Zürich, Switzerland*

(Dated: November 28, 2017)

Tightly focused optical dipole traps induce vector light shifts ("fictitious magnetic fields") which complicate their use for single-atom trapping and manipulation. The problem can be mitigated by adding a larger, real magnetic field, but this solution is not always applicable; in particular, it precludes fast switching to a field-free configuration. Here we show that this issue can be addressed elegantly by deliberately adding a small elliptical polarization component to the dipole trap beam. In our experiments with single ^{87}Rb atoms laser-cooled in a chopped trap, we observe improvements up to a factor 11 of the trap lifetime compared to the standard, seemingly ideal linear polarization. This effect results from a modification of heating processes via spin-state diffusion in state-dependent trapping potentials. We develop Monte-Carlo simulations of the evolution of the atom's internal and motional states and find that they agree quantitatively with the experimental data. The method is general and can be applied in all experiments where the longitudinal polarization component is non-negligible.

I. INTRODUCTION

When a linearly polarized electromagnetic beam is focussed so tightly that the paraxial approximation breaks down, its polarization near the focus is no longer purely transverse, but acquires a longitudinal component that increases with the confinement of the field and leads to polarization gradients in the strongly confined region. The effect has been known for a long time [1], but currently gains importance in the context of light-matter interfaces with ultracold atoms. While similar effects play an enabling role in the new field of chiral quantum optics [2], they complicate the use of strongly focussed, far-detuned laser beams for trapping and manipulating single atoms. Such single-atom tweezers [3] are a powerful tool with many applications. They have been used, for example, to prepare a single trapped atom by collisional blockade [3], to entangle single atoms by Rydberg blockade [4, 5], to laser cool a single atom to its vibrational ground state [6, 7], and to couple an atom to a near-field optical structure [8]. When realized with a pigtailed optical fiber, a single-atom tweezer also enables an attractively simple source of narrowband single photons [9].

For standard dipole traps, the polarization is commonly chosen to be linear to ensure an equal light shift for all magnetic sublevels of the ground state [10]. In single-atom tweezer experiments, where tight focussing is mandatory, the atom experiences an elliptical polarization with spatial variations on the wavelength scale even for a linearly polarized input field. The result is a vector light shift, which depends on the magnetic quantum number and can be described by a an effective, "fictitious" magnetic field [11]. Fictitious magnetic field gradients in combination with diffusion between Zeeman sub-states of the atoms induced by some near-resonant light are detrimental as they lead to heating mechanisms that prevent efficient cooling and reduce trap lifetime [6, 7]. While an actual compensation of fictitious magnetic field gradients has been achieved for nanofiber-based dipole traps using counter-propagating fields [12, 13], this is difficult to realize in other optical microtraps. The approach that has been followed so far with optical tweezers is to mitigate the effect by adding a stronger, real magnetic field in a direction orthogonal to the fictitious field in order to reduce the field gradient [6, 7]. It is however not always possible to add strong real magnetic fields, whose switching dynamics are usually slow.

In this article, we experimentally demonstrate that a properly chosen non-linear input polarization can be used instead of a real magnetic field to mitigate the damaging effects of vector light shift gradients. Our single-atom tweezer is chopped at rather high frequencies up to 4 MHz. In this way, spectroscopy, optical cooling and single-photon generation can be performed on an unperturbed atom during the field-free periods, while still providing a strong effective trapping potential [9, 14, 15]. As we show, a slightly elliptical polarization for the input field of the chopped tweezer can improve the lifetime of the trapped and laser-cooled atom by more than an order of magnitude. This is against the common belief that linear polarization is the best choice for an optical dipole trap [16], which actually holds only as long as the longitudinal component of the electromagnetic field and Zeeman sub-states diffusion can be neglected. We analyze how the experimental lifetime of the trapped atom depends on the trap chopping frequency and on the dipole trap light polarization. We then develop a model based on trap modifications due to quantum jumps between different Zeeman sub-states of the atom and perform Monte-Carlo simulations in very good agreement with the experimen-

* sgarcia@phys.ethz.ch

† long@lkb.ens.fr

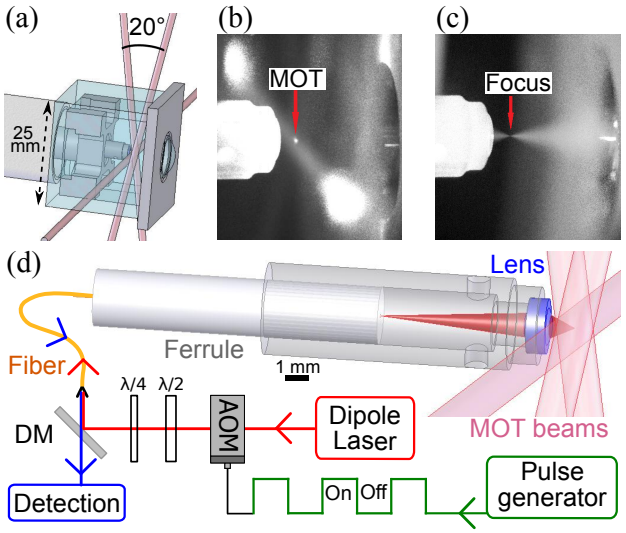

FIG. 1. (a) Experimental setup: the fiber-pigtailed optical tweezer is placed inside a cubic 25 mm size all-glass cell. To load the dipole trap, we produce a cloud of laser-cooled atoms in a MOT with three retro-reflected 1 mm diameter beams, two of them crossing at an angle of 20 deg to avoid clipping at the lens. (b) Image by fluorescence of a ^{87}Rb atomic cloud in the MOT. For this image, the rubidium pressure inside the cell has been strongly increased to make the cloud visible. (c) With the same high-level pressure and by sending resonant light at 780 nm in the fiber, we can see the position of the tweezer focus by imaging the fluorescence of the vapor background atoms. As the focus at 810 nm is 2 μm apart, the dipole trap light is well focussed at the center of the MOT. (d) The optical tweezer collects also the resonant photons from trapped single atoms. An acousto-optic modulator (AOM) chops with 50% duty cycle the dipole trap laser whose polarization is controlled by two waveplates .

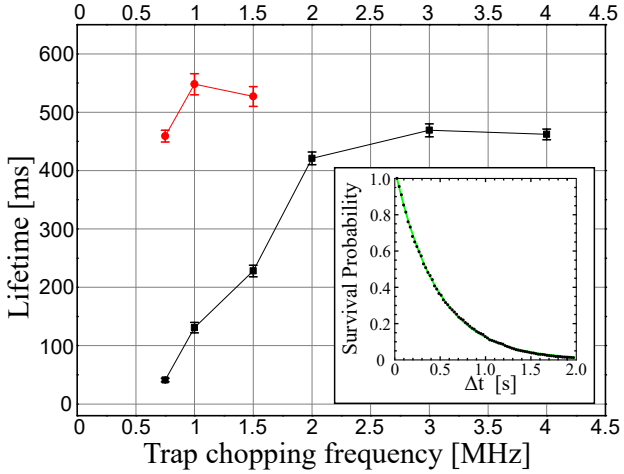

FIG. 2. Observed lifetimes as function of trap modulation frequency for linear polarized dipole trap light (black squares) and for an optimized elliptic polarization with $\alpha_{\rm opt} = 7.0(2)$ deg corresponding to $|C_z| = 0.243(5)$ (red dots). The error bars represent the standard deviation of fitted lifetimes for random exponential distributions with same lifetime and same number of trapped atoms (on the order of 10^3 per point) than the data. Inset: example of lifetime extraction by exponential fit (green) of experimental survival probability decay (black dots) as function of time (Δt) elapsed since the atom entered in the trap, for a linear polarization with 3 MHz chopping frequency.

tal data.

II. MEASUREMENT OF SINGLE ATOM LIFETIME FOR DIFFERENT POLARIZATIONS

In our experimental setup (see Fig. 1) described in detail in Ref. [9], we have developed a miniature and robust fiber-pigtailed optical tweezer, where the same fiber is used to trap a single ^{87}Rb atom and to read-out its fluorescence. We have also demonstrated that, once loaded, the pigtailed tweezer can be used as a single-photon source at 780 nm. To load the tweezer, we produce a laser-cooled atoms cloud in a magneto-optical trap (MOT) at the focus of a far off-resonance optical dipole trap with a wavelength of 810(1) nm and a measured waist of 1.4(1) μm (the number in parentheses is the numerical value of standard uncertainty referred to the corresponding last digits of the quoted result). To eliminate trap-induced light shifts, which reduce the efficiency of the MOT cooling, constitute a source of spectral broadening, and to avoid the generation of 780 nm photons by anti-Stokes Raman scattering of the trapping light inside the fiber, we chop the dipole trap light with a 50% duty cycle using an acousto-optical modulator (see Fig. 1.d) . If the chopping frequency is much larger than twice the largest trap oscillation frequency, the atom is expected to stay trapped in this attractive time-averaged potential. When the dipole trap light is on, the trap depth is 5.6(8) mK, and the calculated transverse and longitudinal trap frequencies are $f_{\rm t} = 167(24)$ kHz and $f_{\rm l} = 22(4)$ kHz.

We have investigated the effect of the chopping frequency on the lifetime of the atom inside the trap (see Fig. 2) in the presence of the MOT beams used to load the dipole trap. The lifetime is obtained by an exponential fit of the survival probability of the atom versus the duration of the trapping. To be mainly limited by background gas collisions, we work in the weak loading regime, where loss due to a second atom entering the trap is negligible. For linearly polarized dipole trap light, the lifetime was limited by background gas collisions at a value of about 500 ms for chopping frequencies above 3 MHz. Below 3 MHz, the lifetime decreases with the chopping frequencies and no single-atom trapping signal could be detected below 500 kHz. So, with this polarization, the chopping frequency needs to be much larger, by about one order of magnitude, than the largest calculated trap frequency. For chopping frequencies between 750 kHz and 1.5 MHz, we observe a strong improvement of the lifetime by adding a small circular component to the polarization of the dipole trap light. The lifetime is

found optimal for an elliptical polarization characterized by the angle $\alpha_{\rm opt} = \arctan(E_b/E_a) = 7.0(2)\,\deg$, where E_a and E_b are the semi-major and semi-minor axes of the electric-field ellipse, respectively. At a chopping frequency of 750 kHz, the lifetime is improved by a factor 11.

These results cannot be explained by the chopping of the dipole trap light, which is expected to be negligible when the trap chopping frequency $f_{\rm m}$ becomes higher than the largest parametric heating frequency $(2f_{\rm t})$ of the trap [17]. Moreover, this effect applies to all polarization configurations and so cannot explain the improved lifetime observed for slightly elliptical polarization. So, we can deduce from these results that additional heating mechanisms reduce the lifetime for a linearly dipole trap light and that this effect can be compensated by using an elliptical polarization.

III. EFFECT OF THE POLARIZATION ON THE OPTICAL TRAPS FOR THE DIFFERENT ZEEMAN SUB-LEVELS

The modification of the lifetime induced by polarization finds its origin in the dipole potential of the ground state which depends on the Zeeman sub-level the atom occupies. For a dipole trap light frequency close to the D1 and D2 transition frequencies of an alkali atom, this potential is given by [7, 18]:

$$U_{\rm dip}\left(\boldsymbol{r}\right) = U_{\rm dip,0}\left(\boldsymbol{r}\right)\left(1 + \frac{\delta_1 - \delta_2}{2\delta_1 + \delta_2}\boldsymbol{C}\left(\boldsymbol{r}\right).\frac{g_F}{\hbar}\hat{\boldsymbol{F}}\right) \qquad (1)$$

$$\text{with} \quad U_{\rm dip,0}\left(\boldsymbol{r}\right) = \frac{\hbar\Gamma}{24}\left(\frac{\Gamma}{\delta_1} + 2\frac{\Gamma}{\delta_2}\right)\frac{I\left(\boldsymbol{r}\right)}{I_{\rm S}} \qquad (2)$$

the scalar dipole potential. In these equations, Γ is the natural linewidth of the excited P levels, $\delta_i = \omega_{\rm L} - \omega_i$ are the detunings between the laser and the D1 and D2 transition frequencies ($i = 1, 2$ respectively), $I\left(\boldsymbol{r}\right)$ the light intensity and $I_{\rm S}$ the saturation intensity. We note $\hat{\boldsymbol{F}}$ the atom angular momentum operator (norm $F = 2$ here) and $g_F = [F(F+1) - I(I+1) + J(J+1)]/[F(F+1)]$. $\boldsymbol{C}\left(\boldsymbol{r}\right) = \Im\left(\boldsymbol{e}_{\rm p}\left(\boldsymbol{r}\right) \times \boldsymbol{e}_{\rm p}\left(\boldsymbol{r}\right)^*\right)$ is a vector characterizing the ellipticity and direction of the polarization represented by a unit vector $\boldsymbol{e}_{\rm p}\left(\boldsymbol{r}\right)$. For a polarization $\boldsymbol{e}_{\rm p} = i\sin(\alpha)\boldsymbol{e}_x + \cos(\alpha)\boldsymbol{e}_y$, we have $\boldsymbol{C} = \sin(2\alpha)\boldsymbol{e}_z$: for linear polarization $\boldsymbol{C} = \boldsymbol{0}$, and for a circular polarization $\|\boldsymbol{C}\| = 1$. When $\boldsymbol{C}$ is non-zero, the different m_F sub-levels experience different light-shifts that are analogous to energy shifts induced by a fictitious magnetic field given by:

$$\boldsymbol{B}_{\mathbf{fict}}\left(\boldsymbol{r}\right) = -U_{\rm dip,0}\left(\boldsymbol{r}\right)\frac{|\delta_1 - \delta_2|}{2\delta_1 + \delta_2}\frac{g_F}{\mu_{\rm B} g_{{\rm L},F}}\boldsymbol{C}\left(\boldsymbol{r}\right), \qquad (3)$$

where $\mu_{\rm B}$ is the Bohr magneton and $g_{{\rm L},F}$ is the Landé g-factor, which is equal to g_F in the usual limits where the electron spin, electron orbital and nuclear Landé g-factors are approximated to $g_{{\rm L},S} \simeq 2$, $g_{{\rm L},L} \simeq 1$ and $g_{{\rm L},I} \simeq 0$, respectively.

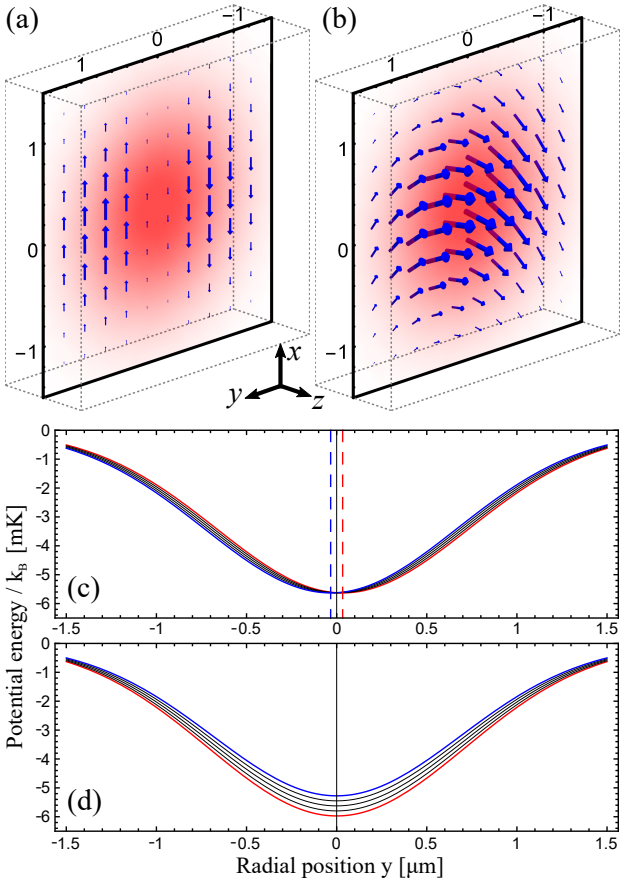

FIG. 3. Dipole potential in the fiber-pigtailed tweezer: (a) Representation of the vector $\boldsymbol{C}\left(\boldsymbol{r}\right)|U_{\rm dip,0}\left(\boldsymbol{r}\right)|$, which is opposite of the fictitious magnetic field $\boldsymbol{B}_{\mathbf{fict}}$ by blue vectors in the xy focal plane (the beam propagates towards increasing values of z) for a linear polarization aligned with the y-axis. The red density plot represents the scalar dipole potential. (b) Same as in (a) for optimal-lifetime elliptic polarization. (c) Dipole potentials of the five Zeeman sub-levels from $m_F = -2$ (red) to $m_F = 2$ (blue) of the $F = 2$ ground state for a linear polarization aligned with the y-axis. The traps are mainly displaced by a regular interval (the trap centers of the extreme states are indicated by dashed vertical lines). (d) Same as in (c) for the case of the optimal-lifetime elliptic polarization. In this case, the trap depths and the oscillation frequencies are modified.

In our optical tweezer, a Gaussian beam is strongly focussed down to a waist $w_0 = 1.4(1)\,\mu$m. For such a diverging beam, a purely transverse incident light (which is linearly-polarized along the y-axis) generates at the focus plane strong variations of the local polarization due to interferences of the different focused light rays. The local $\boldsymbol{C}\left(\boldsymbol{r}\right)$ characteristic vector is calculated via vector Debye integral [1] and we plot the product $\boldsymbol{C}\left(\boldsymbol{r}\right)|U_{\rm dip,0}\left(\boldsymbol{r}\right)|$, which is opposite of the fictitious magnetic field in our case, on Fig. 3.a. The effect is well approximated by a

gradient $C' = 0.267(36)\,\mu\text{m}^{-1}$ of the $\boldsymbol{C}(\boldsymbol{r}) = (C'y, 0, 0)$ vector. Figure 3.c presents the different potentials of the five m_F sub-levels along the y-axis in our trap by choosing the quantization axis of angular momentum as the unit vector of x-axis. At first order, the traps are displaced with state-dependent trap centers:

$$y_c(m_F) = \frac{w_0^2}{4}\frac{\delta_1 - \delta_2}{2\delta_1 + \delta_2} C' g_F m_F = -m_F \times 16.7(8)\,\text{nm}\ . \tag{4}$$

We can see on Fig. 3.a that an atom crossing the x-axis while maintaining its spin will see a flip of the orientation of the fictitious magnetic field. This situation is analogous to the evolution of atom spins crossing the center of a linear magnetic trap. In our linearly polarized dipole trap, the scalar potential provides an additional confinement which leads only to a displacement of the trap centers instead than spin flip losses.

If a large circular component is present in the polarization of the dipole trap light before the focus, it will induce a strong uniform z-component of the $\boldsymbol{C}$ vector, which will dominate over the linear polarization gradients, making them negligible. The dipole potential is then given by :

$$U_{\text{dip}}(\boldsymbol{r}, m_F) = U_{\text{dip},0}(\boldsymbol{r})\left(1 + \frac{\delta_1 - \delta_2}{2\delta_1 + \delta_2} g_F m_F \|\boldsymbol{C}\|(\boldsymbol{r})\right) \tag{5}$$

where the quantization axis of the angular momentum is chosen in the direction of the local $\boldsymbol{C}$ vector. The traps of the different sub-levels have the same center, but differ in trap depth and oscillation frequencies, as shown by Fig. 3.d. This effect increases with the weight of the circular component of the polarization. As can be seen in Fig. 3.b, an atom crossing the y-axis will experience a continuous evolution of the orientation of the fictitious magnetic field whose variation decreases when the circular component increases. For a large enough circular component, the atom spin will be able to follow adiabatically the orientation of the field.

The natural question is then to determine what is the minimal amount of circular component (i.e. the smallest value of the z-component C_z of the $\boldsymbol{C}$ vector) one needs to add to obtain an adiabatic evolution and thus mitigate the polarization gradient effects. We can estimate a lower bound for C_z by using the criterion for adiabatic evolution of the spin given by $\omega_L \gg |\text{d}\theta/\text{d}t|$ where ω_L is the Larmor precession angular frequency and $|\text{d}\theta/\text{d}t|$ is the change of the orientation angle θ of the field during the atom motion. Considering that $\boldsymbol{C} = (C'y, 0, C_z)$ define the angle θ and using an harmonic approximation for the trap, one finds that the maximum of angle variation is obviously in the center of the trap where the atom speed v_y is maximum and is given by $|\text{d}\theta/\text{d}t| = |C'/C_z|\,|v_y|$. In the range of low values of $|C_z|$ that we consider here, the Larmor precession angular frequency has a local minimum in the middle of the trap with value $\omega_L = \frac{U_{\text{dip},0}(\boldsymbol{0})}{\hbar} g_F \frac{\delta_1 - \delta_2}{2\delta_1 + \delta_2}\,|C_z|$. The evolution thus becomes adiabatic when the circular component fulfills:

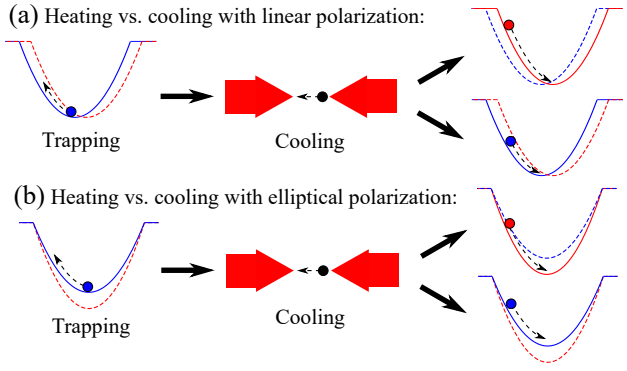

FIG. 4. Simplified schemes (with only two spin states represented in red and blue) of the cycles followed by the trapped atom. The MOT cooling when the dipole trap is off competes with the heating of trap potential fluctuations induced by the spin-state quantum jumps.

$$|C_z| \gg \sqrt{\frac{\hbar |C'||v_y|}{U_{\text{dip},0}(\boldsymbol{0})\, g_F \frac{\delta_1 - \delta_2}{2\delta_1 + \delta_2}}}. \tag{6}$$

For our optical tweezer, we find that $|C_z| \gg 0.018$ by estimating the maximum speed v_y at the center of an harmonic trap with by $v_y = \sqrt{2k_B T_D / m_{\text{Rb}}}$, where m_{Rb} is the ^{87}Rb atom mass and $T_{\text{D}} \simeq 140\ \mu$K the Doppler temperature. We find indeed experimentally that for our optimal polarization $|C_z| = 0.243(5)$. This is one order of magnitude larger than the estimated lower bound, ensuring an adiabatic evolution of the spin, that minimizes the effect of state-dependent trap centers induced by the polarization gradient.

IV. HEATING MECHANISMS

In order to get a better understanding, we identify different heating processes of the trapped single atom that compete with the cooling provided by the MOT beams. For the linear and elliptic polarization configurations, they originate from the change of spin sub-level m_F due to the excitation by the MOT beams and desexcitation to the ground state. The evolution of an atom is schematically represented by Fig. 4, for the linear and elliptic polarizations, respectively. When the dipole trap is on, light shifts are so large (117(18) MHz at the center) that the excitation by the MOT beams can be neglected, and the atom oscillates freely in the trap while conserving its spin state. When the dipole trap is switched off, the MOT beams become almost resonant and provide both cooling and spin state transitions. When the dipole trap laser is switched on again, the quantum jumps of the spin-state may have led the atom to a different m_F-state and so to experience a different trap. We have then three different heating mechanisms :

- for any polarization: when the dipole trap is off, the atom can escape by spatial diffusion. This process is negligible if the chopping frequency is much larger than twice the largest trap oscillation frequency.
- for linear polarization: the spin-state diffusion gives rise to a random trap shaking due to the displacement of the state-dependent trap centers.
- for elliptical polarization: the spin-state diffusion leads to heating by a random modulation of the trap frequencies.

The different heating effects are larger for lower chopping frequencies, because the atom evolves longer in the trap and in the MOT between two changes, which gives larger energy differences. An optimal elliptic polarization exists mitigating the heating by random trap shaking in the linearly polarized beam and the heating by random trap-frequency modulation for moderate elliptic polarization, while the modulation amplitude of the latter increases with the weight of the circular component.

In dipole traps with large waist, polarization gradients are negligible and only trap-frequency modulation induced by elliptical polarization limits the lifetime. The best polarization is then the linear one that cancels this effect [16]. If polarization gradients cannot be neglected, the two last heating mechanisms will be present whenever spin-state diffusion occurs even for static trap. This is specially the case for every experiment where cooling of the atoms by near-resonant light is undertaken [6, 7]. In this case, a non-zero polarization minimizing the heating exists. Our experimental situation emphasizes the effect of spin-state diffusion by using a chopped trap where the cooling light is nearly resonant light when the trap is switch off.

V. SIMULATION OF SINGLE ATOM LIFETIME

To confirm the above explanation of the observed lifetime evolution with the trap modulation frequency in terms of trap modifications implied by quantum jumps of spin state, we perform Monte-Carlo simulations of the atom motion in our pulsed trap. For a given polarization, the simulation considers the evolution of several thousands of atoms subjected to about a million cycles of alternating trapping and cooling phases. In order to obtain realistic computational times, we make some approximations that simplify the calculations while keeping the main physical features of the experimental situation.

The first approximation consists in limiting the simulation to two dimensions given by the strong axes of the trap (transverse to the dipole trap laser propagation axis) which have oscillation frequencies an order of magnitude higher than the weak axis one. Thus, the energy change during one modulation cycle is much more important along these axes. We also consider truncated harmonic traps which provide a good approximation of the Gaussian potential in the center where the atom mostly evolves, and which have a depth limited by the maximum dipole trap light shift. For a linear polarization, the state dependent traps are shifted along the y-axis by $y_c\,(m_F)$ (cf. Eq 4). For an elliptic polarization, we change the trap depth and frequencies according to Eq. 5.

The exact treatment of the cooling in 6 nearly resonant MOT beams implies to know the 5 relative phases between the beams and to resolve the 78 coupled optical Bloch equations. We simplify this description by taking an usual classical damping force $-m_{\mathrm{Rb}}\gamma_v \boldsymbol{v}$ where γ_v is the characteristic damping coefficient. In our setup, the cooling on the y-axis is stronger. Due to geometrical hindrance, two pairs of MOT beams have indeed a 10 deg deviation from this axis, so we use here a damping coefficient $2\cos(10\,\mathrm{deg})\gamma_v$. The Doppler cooling limit is considered by canceling this force if the atom kinetic energy is lower than the thermal energy $k_{\mathrm{B}}T_{\mathrm{D}}$ at the Doppler temperature when the cooling phase starts. To approximately describe the change in m_F spin state of the atom, we calculate, from the Clebsch-Gordan coefficients, the probabilities of excitation to the different sub-levels of the $5^2P_{3/2}$ $F'=3$ excited state in an isotropic light field and the probabilities of spontaneous emission down to the $5^2S_{1/2}$ $F=2$ sub-levels. It gives us the probabilities to change from a state to another per photon scattering event. For a given initial state, the final state probabilities after the cooling phase are then given by its duration $\tau_{1/2}=1/(2f_{\mathrm{m}})$, the average scattering rate Γ_{ch} and the analytic solution of the coupled equations of state population evolution. These two parameters γ_v and Γ_{ch} of the cooling phase are difficult to estimate carefully in our system because we need intense MOT beams ($50\ \mathrm{mW/cm^2}$) to provide efficient trap loading, thus we can not apply the usual low saturation limit. Nevertheless, an heuristic equation established in Ref. [19] (Eq. 4) and the measured rate of spontaneously emitted photons in the detection respectively give some approximate initial values of γ_v and Γ_{ch}. These values are then adjusted to fit the experimental data. We find $\gamma_v = 3.3\,\mathrm{kHz}$ which is 30% lower that the initial value, and with $\Gamma_{\mathrm{ch}} = 35\,\mathrm{MHz}$ that is roughly three time higher than the observed spontaneous emission. The latter result can be explained by the fact that we are using beam intensities well above the saturation, where stimulated emission processes dominate.

We initiate a simulation by picking an atom in $m_F = 0$ state and randomly distributed in phase space with a Gaussian density probability characterized by the Doppler temperature T_{D} and the trap frequency. We start the first cycle by the trapping phase and calculate the position and speed after a chopping period half $\tau_{1/2}$ of evolution. Then, we let the atom move under the cooling force for another $\tau_{1/2}$. Afterward, we randomly change the internal state according to the calculated probabilities and reckon the atom energy from its state, position and speed in the dipole trap. We repeat this cycle until the atom energy reaches a value higher than the trap depth (which means that it escapes from the trap) or

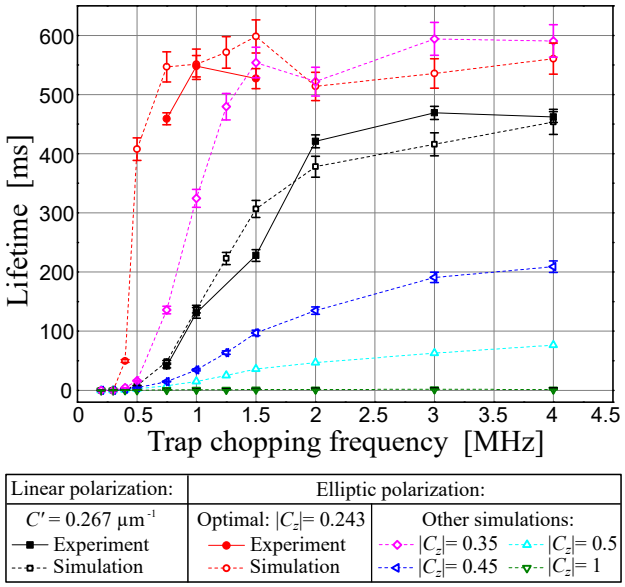

FIG. 5. Results of lifetime as function of trap pulsing frequency given by atomic motion simulations for different dipole trap light polarization with 500 simulated atoms for each point. The error bars represent the 4.7% relative standard deviation for 500 events of an exponential distribution.

until the time exceeds a random value from an exponential distribution. The latter takes into account the background gas collisions which limit the atom lifetime to 550 ms according to the experimental data.

By using the simulation without spin state changes, we first verified that the heating due to the chopping of the dipole trap is negligible for chopping frequencies higher than 400 kHz, as expected since $2f_t \simeq 340$ kHz. For the different polarization configurations in presence of spin-state diffusion, the lifetimes extracted from the survival probabilities of 500 simulated atoms are presented on Fig. 5. The results show the improvement of the lifetime that was observed experimentally for an elliptic polarization with a small circular component compared to a linear polarization, and agree quantitatively well with the experimental data. As a larger circular polarization component of the dipole trap light is added ($|C_z|$ increasing), the lifetime decreases and almost cancels for a pure circular polarization even for large modulation frequencies. This explains why we were not able to detect any atom for large circular components in the polarization of the dipole trap light. These simulations confirm the existence of an optimal elliptic polarization that limits heating due to atom spin state quantum jumps in high NA tweezers.

VI. CONCLUSION AND OUTLOOK

We have shown how some deleterious effects of polarization gradients in strongly focused optical tweezers can be mitigated by using elliptical polarization of the incoming dipole trap light. This method is general and can be applied in any experiment where the light field is tightly confined so that the longitudinal component of the polarization is non-negligible and where spin-state diffusion occurs due to the presence of near-resonant light, required for example to cool the atoms inside the traps. Besides strongly focused optical tweezers, this also includes optical nanofiber [20] and optical microcavities [21, 22].

ACKNOWLEDGMENTS

We acknowledge funding from the ANR SAROCEMA project, grant ANR-14-CE32-0002 of the French Agence Nationale de la Recherche and from Émergence-UPMC-2009 research program. We thank D. Maxein and L. Hohmann for contributions in the early stage of the experiment.

[1] B. Richards and E. Wolf, Proceedings of the Royal Society of London A: Mathematical, Physical and Engineering Sciences **253**, 358 (1959).
[2] P. Lodahl, S. Mahmoodian, S. Stobbe, P. Schneeweiss, J. Volz, A. Rauschenbeutel, H. Pichler, and P. Zoller, Nature **541**, 473 (2017).
[3] N. Schlosser, G. Reymond, I. Protsenko, and P. Grangier, Nature **411**, 1024 (2001).
[4] E. Urban, T. A. Johnson, T. Henage, L. Isenhower, D. D. Yavuz, T. G. Walker, and M. Saffman, Nature Physics **5**, 110 (2009).
[5] A. Gaëtan, Y. Miroshnychenko, T. Wilk, A. Chotia, M. Viteau, D. Comparat, P. Pillet, A. Browaeys, and P. Grangier, Nature Physics **5**, 115 (2009).
[6] A. M. Kaufman, B. J. Lester, and C. A. Regal, Phys. Rev. X **2**, 041014 (2012).
[7] J. D. Thompson, T. G. Tiecke, A. S. Zibrov, V. Vuletić, and M. D. Lukin, Phys. Rev. Lett. **110**, 133001 (2013).
[8] J. D. Thompson, T. G. Tiecke, N. P. de Leon, J. Feist, A. V. Akimov, M. Gullans, A. S. Zibrov, V. Vuletic, and M. D. Lukin, Science **340**, 1202 (2013).
[9] S. Garcia, D. Maxein, L. Hohmann, J. Reichel, and R. Long, Applied Physics Letters **103**, 114103 (2013).
[10] R. Grimm, M. Weidemüller, and Y. B. Ovchinnikov, Advances in atomic, molecular, and optical physics **42**, 95 (2000).
[11] C. Cohen-Tannoudji and J. Dupont-Roc, Phys. Rev. A **5**, 968 (1972).
[12] A. Goban, K. S. Choi, D. J. Alton, D. Ding, C. Lacroûte, M. Pototschnig, T. Thiele, N. P. Stern, and H. J. Kimble, Phys. Rev. Lett. **109**, 033603 (2012).
[13] B. Albrecht, Y. Meng, C. Clausen, A. Dareau, P. Schneeweiss, and A. Rauschenbeutel, Phys. Rev. A

94, 061401 (2016).
[14] S. Chu, J. E. Bjorkholm, A. Ashkin, and A. Cable, Phys. Rev. Lett. **57**, 314 (1986).
[15] N. R. Hutzler, L. R. Liu, Y. Yu, and K.-K. Ni, New Journal of Physics **19**, 023007 (2017).
[16] K. L. Corwin, S. J. M. Kuppens, D. Cho, and C. E. Wieman, Phys. Rev. Lett. **83**, 1311 (1999).
[17] T. A. Savard, K. M. O'Hara, and J. E. Thomas, Physical Review A **56**, R1095 (1997).
[18] S. J. M. Kuppens, K. L. Corwin, K. W. Miller, T. E. Chupp, and C. E. Wieman, Physical review A **62**, 013406 (2000).
[19] W. Wohlleben, F. Chevy, K. Madison, and J. Dalibard, The European Physical Journal D-Atomic, Molecular, Optical and Plasma Physics **15**, 237 (2001).
[20] R. Mitsch, C. Sayrin, B. Albrecht, P. Schneeweiss, and A. Rauschenbeutel, Nature Communications **5**, 5713 (2014).
[21] C. Junge, D. O'Shea, J. Volz, and A. Rauschenbeutel, Phys. Rev. Lett. **110**, 213604 (2013).
[22] I. Shomroni, S. Rosenblum, Y. Lovsky, O. Bechler, G. Guendelman, and B. Dayan, Science **345**, 903 (2014).